**iScience, Volume *25***

## Supplemental information

# Structural and functional analysis of an inter-Spike bivalent neutralizing antibody against SARS-CoV-2 variants

**Yaning Li, Qing Fan, Bing Zhou, Yaping Shen, Yuanyuan Zhang, Lin Cheng, Furong Qi, Shuo Song, Yingying Guo, Renhong Yan, Bin Ju, and Zheng Zhang**

A

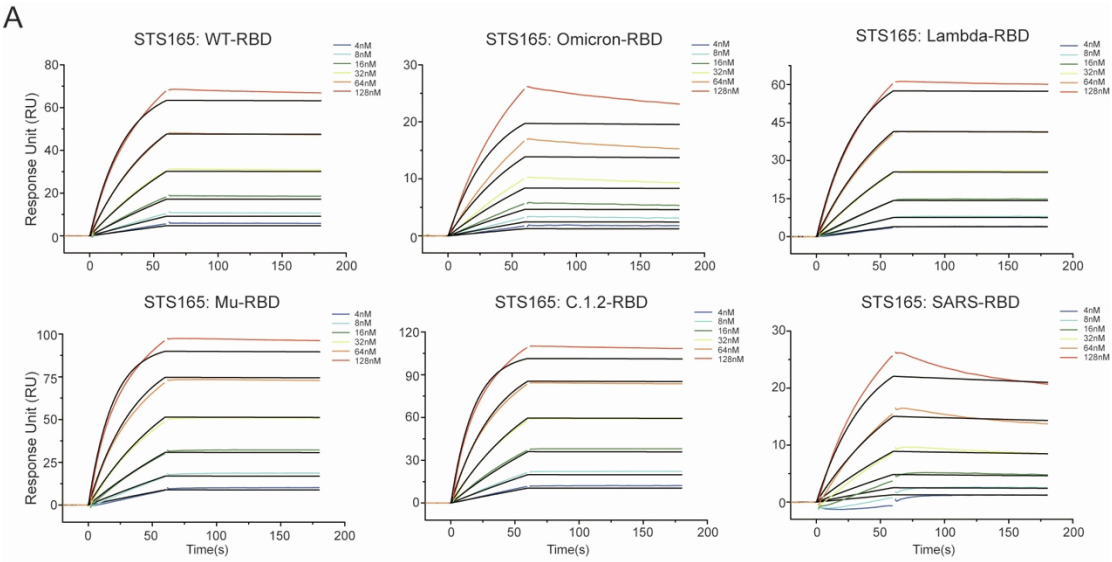


B

| Variants | Ka(M-1·s−1) | Kd(s-1) | KD(nM) |
|---|---|---|---|
| WT-RBD | 1.96E+05 | 1.99E-05 | 0.1021 |
| Omicron-RBD | 2.31E+05 | 8.10E-05 | 0.3520 |
| Lambda-RBD | 2.49E+05 | 2.33E-05 | 0.0938 |
| Mu-RBD | 4.15E+05 | 3.04E-05 | 0.0733 |
| C.1.2-RBD | 4.40E+05 | 2.72E-05 | 0.0619 |
| SARS-RBD | 2.15E+05 | 4.26E-04 | 1.9900 |

**Figure S1: The SPR result of STS165 binding to different variant RBD proteins,** Related to Figure 1

**(A)** Examples of binding affinities of STS165 to RBD of WT, Omicron, Lambda, Mu, C.1.2, and SARS-CoV. **(B)** The affinity values of STS165 to SARS-CoV or different SARS-CoV-2 mutant RBD proteins. Data are means of two independent experiments. The curves are representatives of similar results.

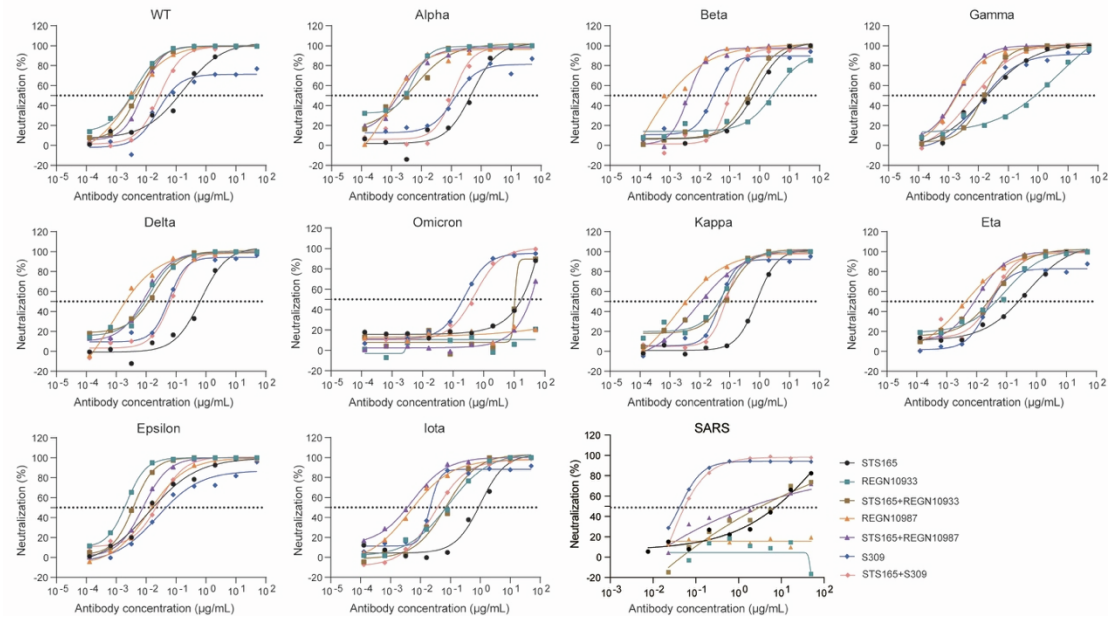


**Figure S2: The neutralization of 11 pseudoviruses by 4 antibodies (STS165, REGN10933, REGN10987, and S309) and antibody cocktails (STS165+REGN10933, STS165+REGN10987, and STS165+S309),** Related to Figure 1

The curves are representatives of at least two independent experiments with similar results.

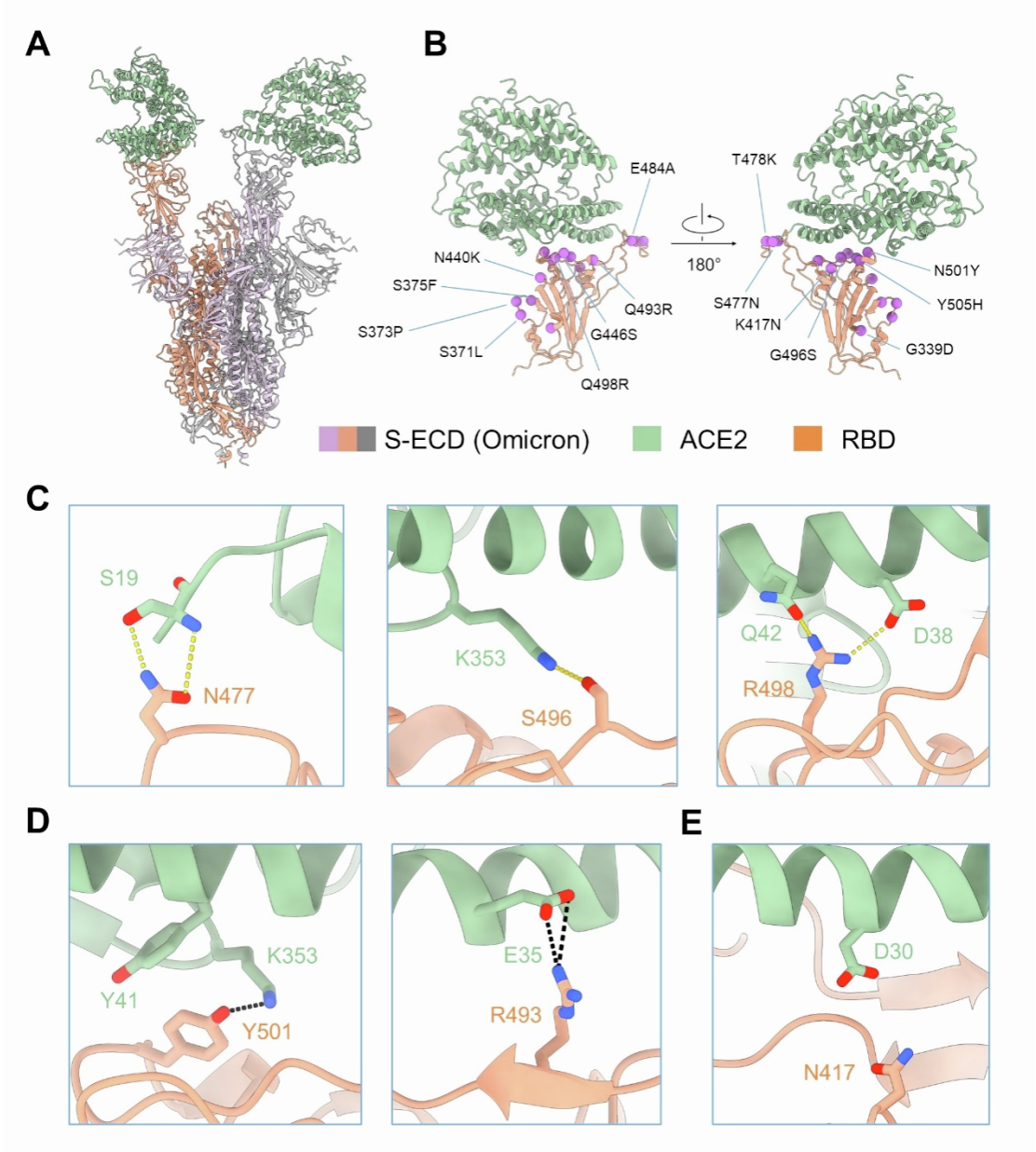


**Figure S3: Cryo-EM structure of S-ECD (Omicron) in complex with PD of ACE2,** Related to Figure 2

**(A)** The domain-colored cryo-EM structure of S-ECD (Omicron) in complex with PD of ACE2 is shown here. PD binds to two "up" RBD, which are colored green. Each of the Spike trimer is colored pink, orange, and grey, respectively. **(B)** The Omicron (RBD) shown in two perpendicular views. Cα of all mutated residues relative to the RBD (Wuhan-Hu-1) are shown as purple sphere. **(C-E)** Change of interactions between Omicron RBD (orange) and ACE2 (green) are shown here. The hydrogen-bond interactions shown as yellow indicate the added interaction, and they

shown as black indicate the alterant interaction. The interaction between D30 of ACE2 and N417 of RBD is broken.

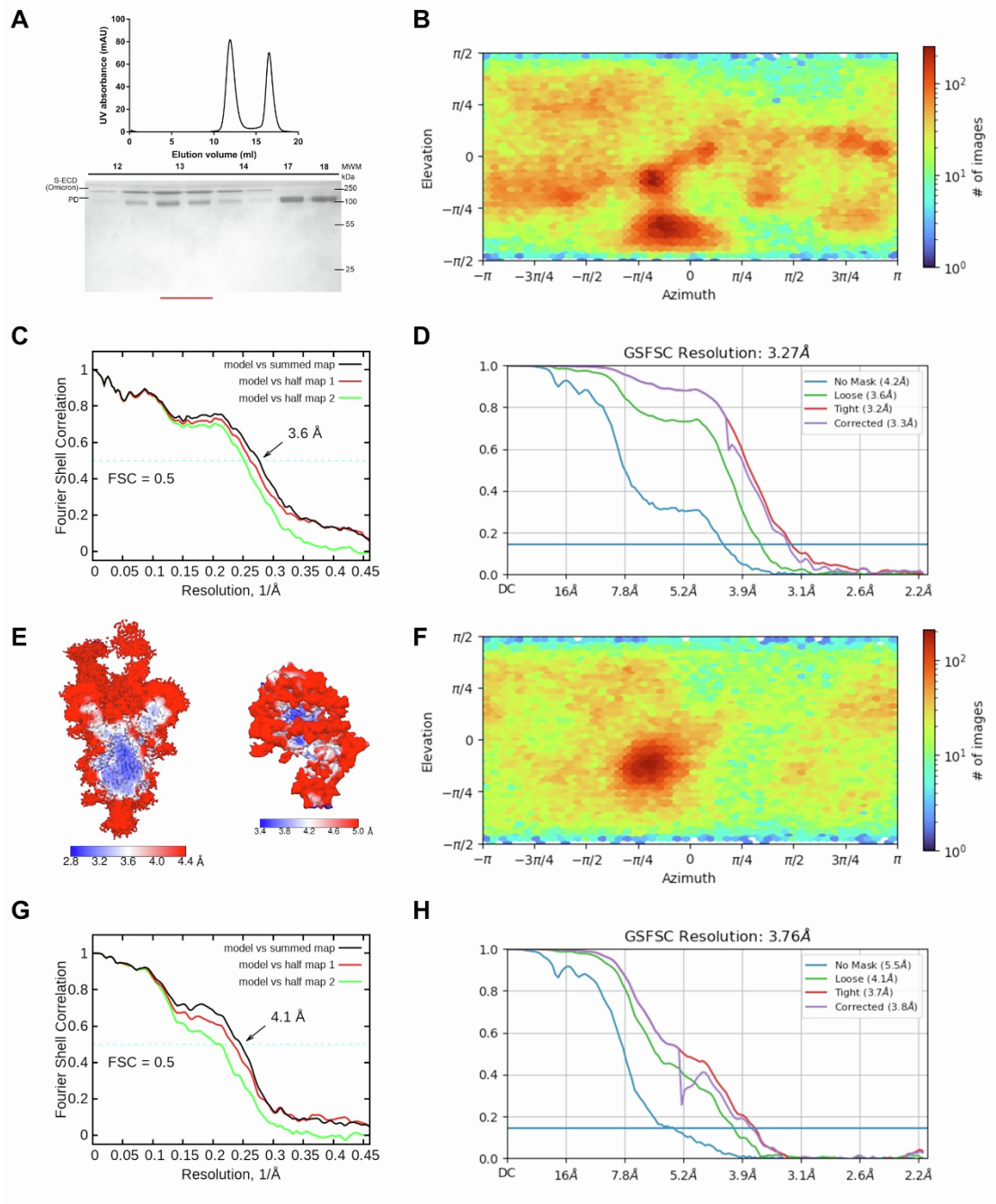


**Figure S4: Cryo-EM analysis of S-ECD (Omicron) in complex with PD of ACE2,** Related to Figure 2

**(A)** Representative SEC purification profile, and fractions for cryo-EM anlysis were marked by red line. **(B)** Euler angle distribution in the final 3D reconstruction of overall map. **(C)** FSC curve of the refined model of S-ECD (Omicron) in complex with PD versus the overall structure that it is refined against (black); of the model refined against the first half map versus the same map (red); and of the model refined

against the first half map versus the second half map (green). The small difference between the red and green curves indicates that the refinement of the atomic coordinates did not suffer from overfitting. **(D)** FSC curve of S-ECD (Omicron) in complex with PD. **(E)** Local resolution map for the 3D reconstruction of overall structure and RBD-PD sub-complex. **(F)** Euler angle distribution in the final 3D reconstruction of RBD-PD sub-complex. **(G)** FSC curve of the refined model of RBD-PD sub-complex versus the overall structure that it is refined against (black); of the model refined against the first half map versus the same map (red); and of the model refined against the first half map versus the second half map (green). The small difference between the red and green curves indicates that the refinement of the atomic coordinates did not suffer from overfitting. **(H)** FSC curve of RBD-PD sub-complex.

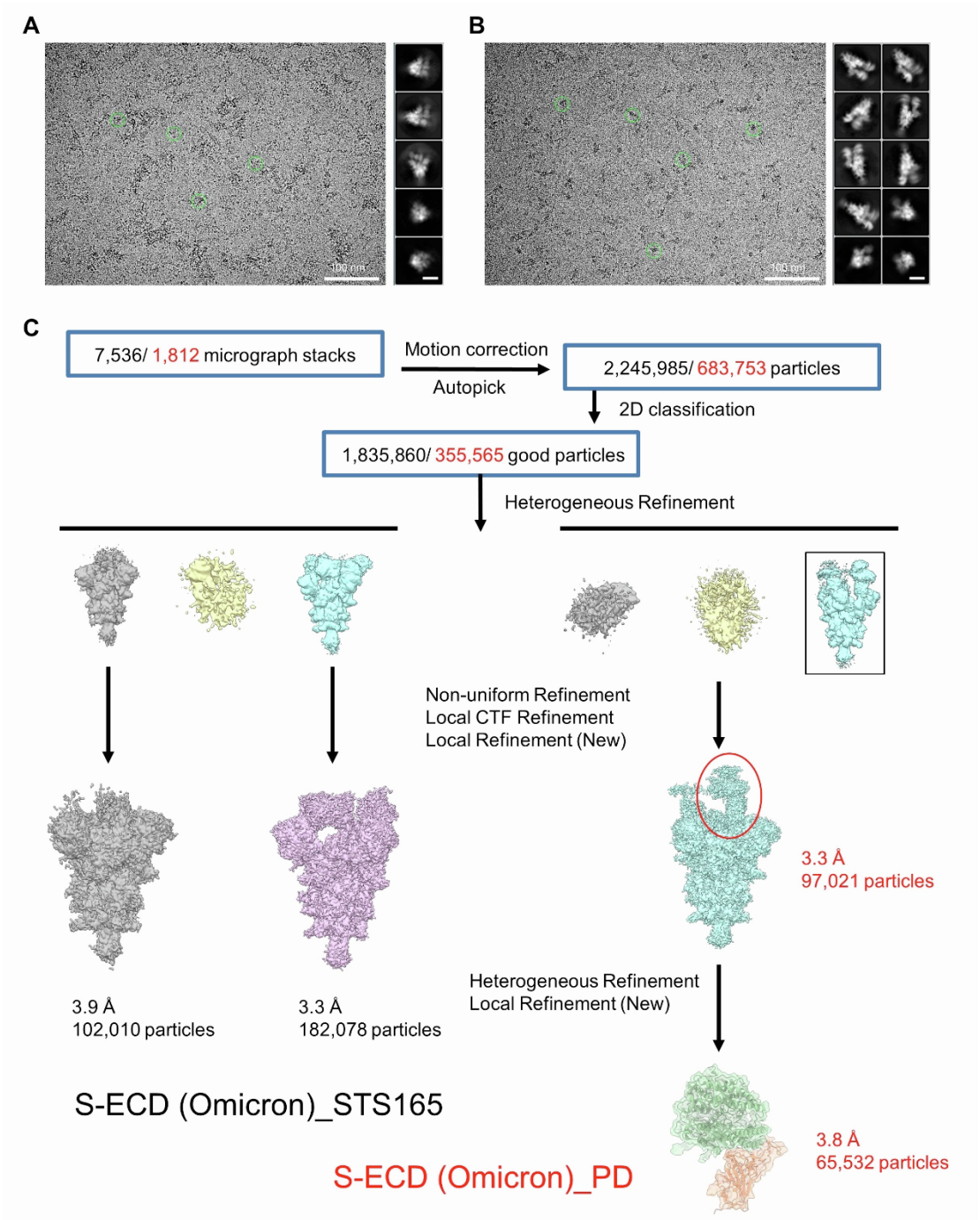


**Figure S5: Flowchart for cryo-EM data processing,** Related to Figure 2

Please refer to the 'Data Processing' in Methods section for details.

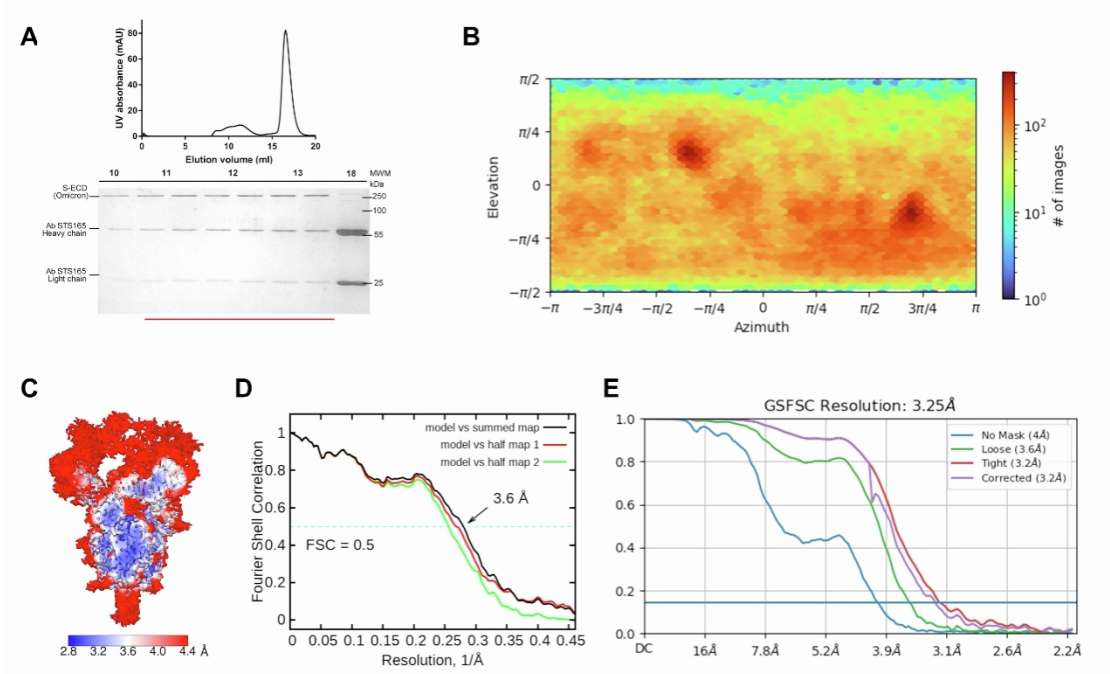


**Figure S6: Cryo-EM analysis of S-ECD (Omicron) in complex with STS165,** Related to Figure 2

**(A)** Representative SEC purification profile, and fractions for cryo-EM anlysis were marked by red line. **(B)** Euler angle distribution in the final 3D reconstruction. **(C)** Local resolution map for the 3D reconstruction of overall structure. **(D)** FSC curve of the refined model of S-ECD (Omicron) in complex with STS165 versus the overall structure that it is refined against (black); of the model refined against the first half map versus the same map (red); and of the model refined against the first half map versus the second half map (green). The small difference between the red and green curves indicates that the refinement of the atomic coordinates did not suffer from overfitting. **(E)** FSC curve of S-ECD (Omicron) in complex with STS165.

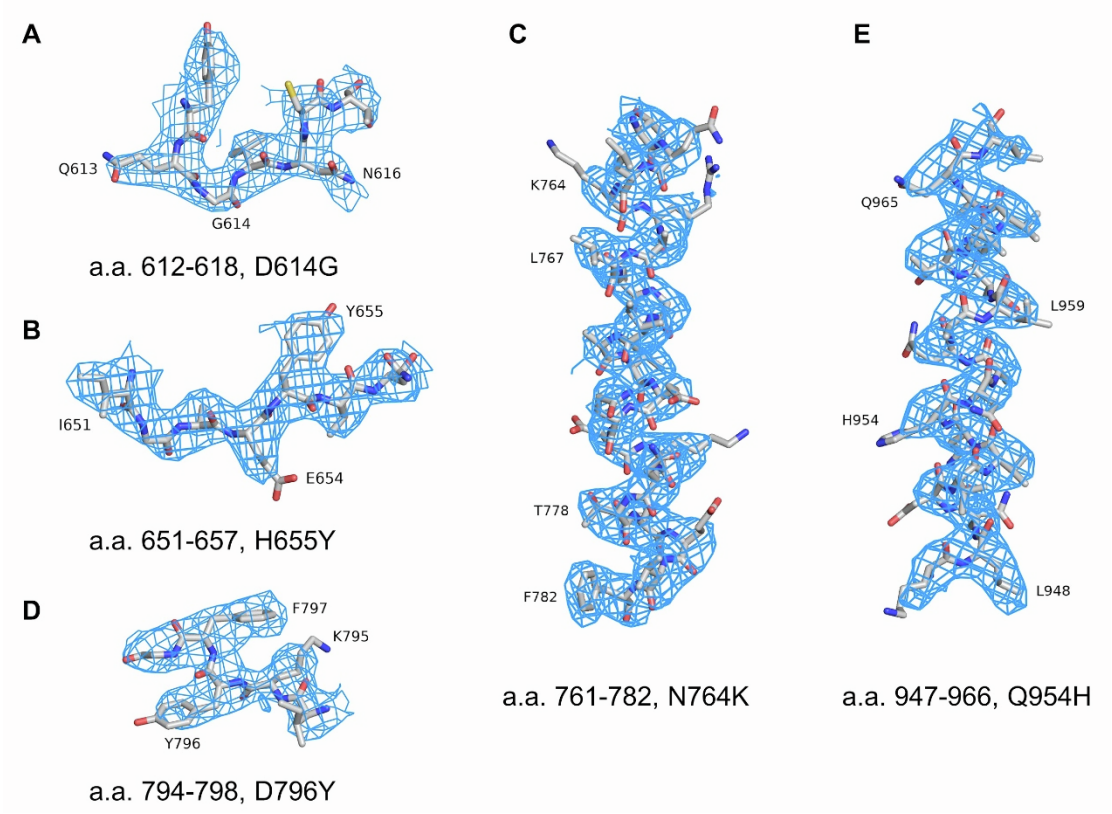


**Figure S7: Representative cryo-EM density maps,** Related to Figure 2

**(A-E)** Cryo-EM density map of S-ECD (Omicron) in complex with STS165 shown at threshold of 7 σ.

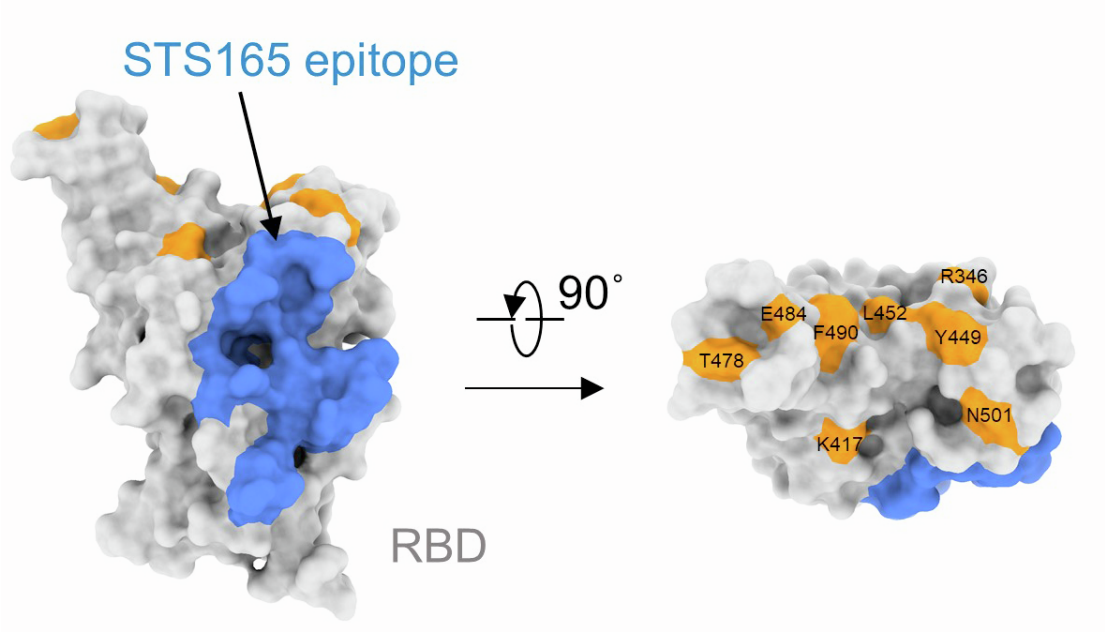


**Figure S8: The binding epitope of STS165 and mutated residues on the RBD of other SARS-CoV-2 variants,** Related to Figure 2

The binding epitope of STS165 bound to the RBD is colored blue on the left, and the mutated residues on the RBD of other SARS-CoV-2 variants, including Alpha, Beta, Gamma, Delta, Lambda, Mu, Kappa, Eta, Epsilon, Iota, and C.1.2 are colored Orange.

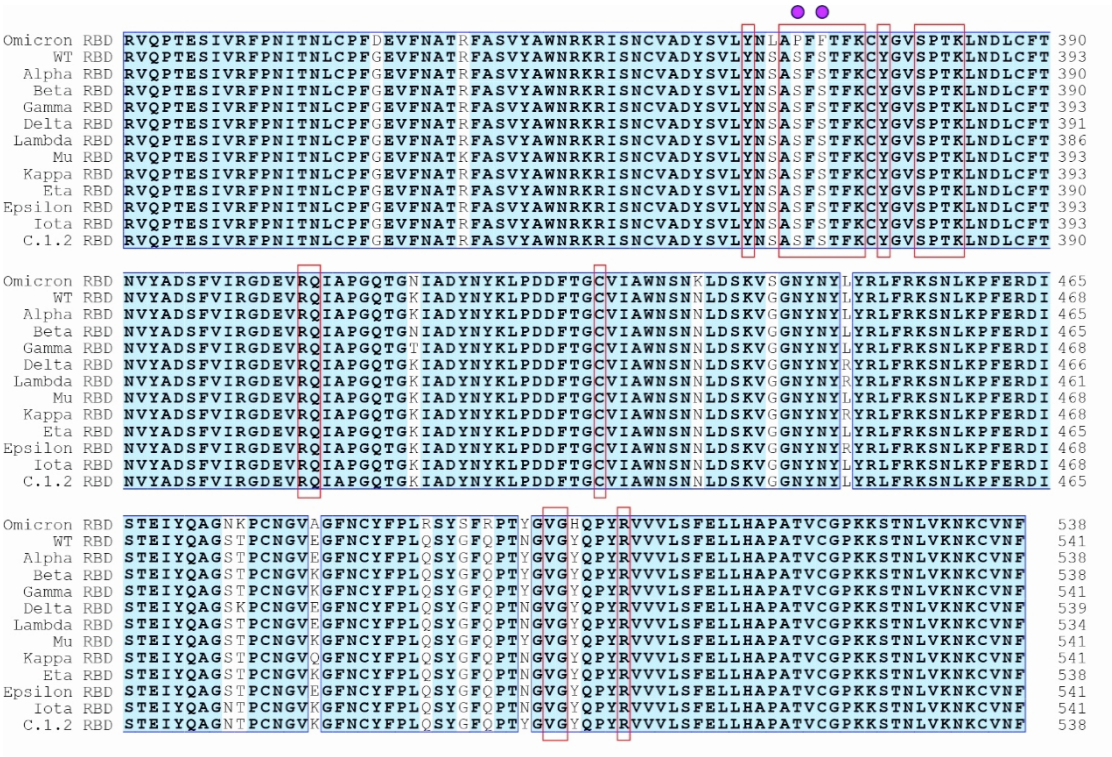


**Figure S9: Sequence alignment of RBD proteins of SARS-CoV-2 variants and SARS-CoV,** Related to Figure 2

The sequences were aligned using clustalX. The thirteen aligned sequences are the RBD of SARS-CoV-2 variants, including Omicron, WT, Alpha, Beta, Gamma, Delta, Lambda, Mu, Kappa, Eta, Epsilon, Iota, and C.1.2. The identical amino acids are colored blue. The binding epitope of STS165 on RBD is lined out by red boxes and the overlaps with the mutated residues relative to the RBD (Omicron) are marked by purple balls.

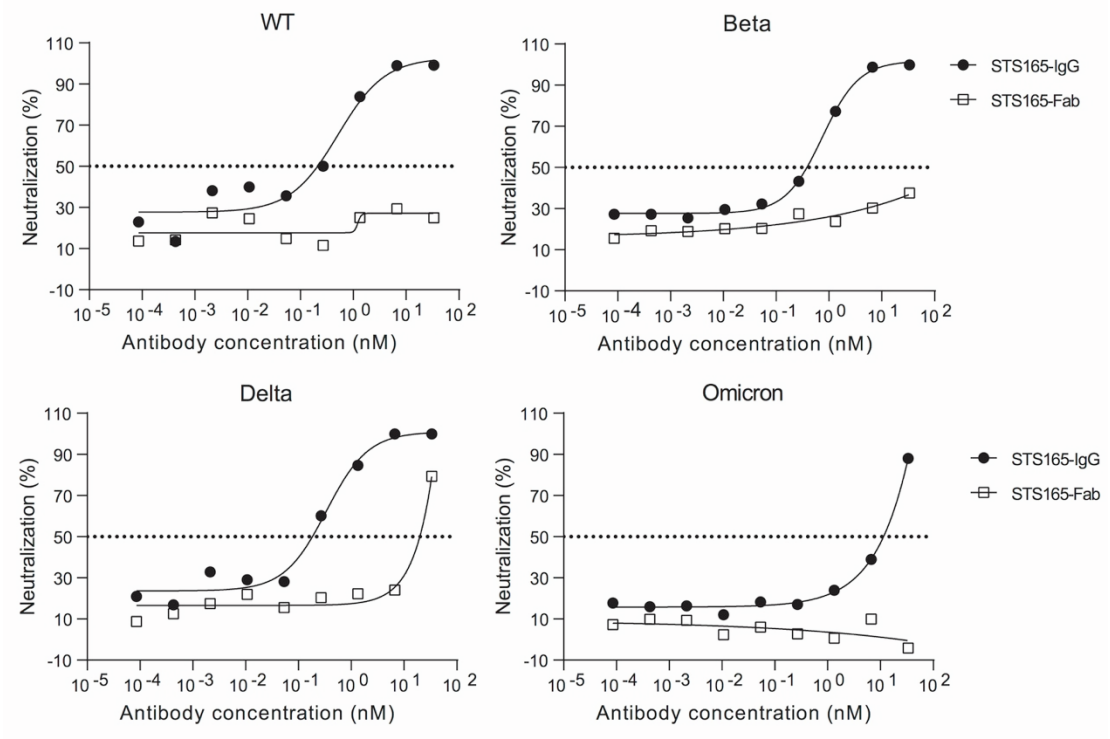


**Figure S10: IgG and Fab form antibody (STS165-IgG and STS165-Fab) neutralize pseudoviruses of WT SARS-CoV-2 and variants (Beta, Delta, and Omicron),** Related to Figure 2

The curves are representatives of two independent experiments with similar results.

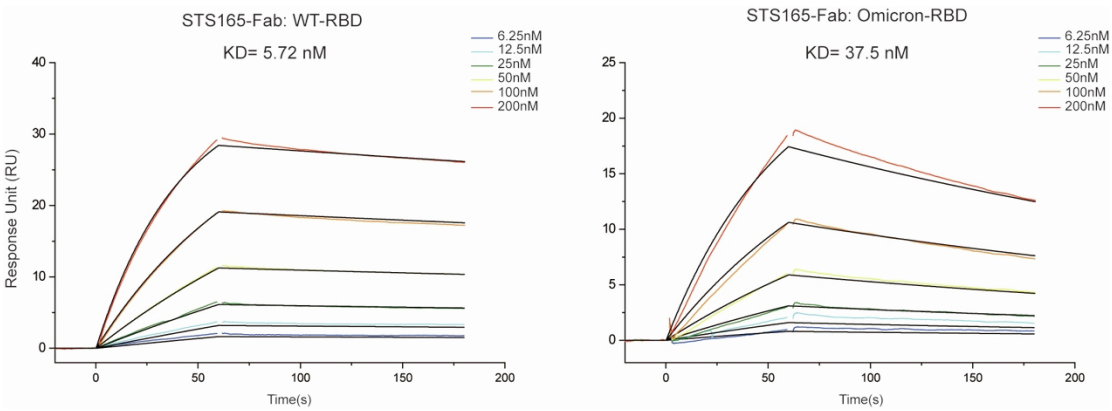


**Figure S11: IgG and Fab form antibody (STS165-IgG and STS165-Fab) bind to RBD proteins of WT SARS-CoV-2 and Omicron variant,** Related to Figure 2

Data are means of two independent experiments. The curves are representatives of similar results.

**Table S1: Data collection, 3D reconstruction and model statistic,** Related to Figure 2

| | | | |
|---|---|---|---|
| **Data collection** | | | |
| EM equipment | Titan Krios (Thermo Fisher Scientific) | | |
| Voltage (kV) | 300 | | |
| Detector | Gatan K3 Summit | | |
| Energy filter | Gatan GIF Quantum, 20 eV slit | | |
| Pixel size (Å) | 1.087 | | |
| Electron dose (e-/Å2) | 50 | | |
| Defocus range (μm) | -1.2 ~ -2.2 | | |
| Sample | S-ECD (Omicron)-STS165 | S-ECD (Omicron)-PD | |
| Number of collected micrographs | 7,536 | 1,812 | |
| **3D Reconstruction** | | | |
| Software | Relion 3.0 | | |
| Sample | Overall | Overall | sub-complex |
| Number of used particles (Overall) | 182,078 | 97,021 | 65,532 |
| Resolution (Å) | 3.3 | 3.3 | 3.8 |
| Symmetry | C1 | | |
| Map sharpening B-factor (Å2) | 113.7 | 101.8 | 138.3 |
| **Refinement** | | | |
| Software | Phenix | | |
| Cell dimensions | | | |
| a=b=c (Å) | 313.056 | | |
| α=β=γ (°) | 90 | | |
| Model composition | | | |
| Protein residues | 3,706 | 4,153 | |
| Side chains assigned | 3,706 | 4,153 | |
| Sugar | 71 | 93 | |
| R.m.s deviations | | | |
| Bonds length (Å) | 0.004 | 0.005 | |
| Bonds Angle (°) | 0.851 | 0.871 | |
| Ramachandran plot statistics (%) | | | |
| Preferred | 93.06 | 92.72 | |
| Allowed | 6.60 | 6.98 | |
| Outlier | 0.34 | 0.30 | |